

# **First tests of a moment autocorrelation method to detect GW from pulsars in binary systems**

**Andrea Viceré – Università degli Studi di Urbino "Carlo Bo" and INFN Firenze, Italy**

**and**

**Michel Yvert – LAPP, Université de Savoie, CNRS/IN2P3, Annecy-le-Vieux, France**

## **Abstract**

The detection of gravitational waves emitted by pulsars in binary systems is a challenge not yet solved. The frequencies of these pulsars are Doppler-shifted due to the relative movement of the two objects, and an optimal detection strategy would require a computing power far beyond the present feasibility. We present here a new approach, which allows reaching a sensitivity potentially good enough to be used as a candidates search (almost for all sky and at all frequencies) thus able to provide a first input to more sophisticated hierarchical detection methods.

We present a test of this new technique using data taken during the first science run of Virgo and injecting in the raw data a set of six simulated pulsars. This method, based on the autocorrelation of the moments' distributions, allows finding the frequency of an eventual pulsar and the period of the system to which it belongs. The computing time needed is found to evolve almost linearly with the amount of input data, a very promising feature.

This work needs to be optimized, it is presented here to point out a possible new road toward the solution of this difficult, but very important, detection problem.

## **1. Introduction**

The detection of Gravitational waves signals emitted by pulsars belonging to binary systems is a problem that has been studied several times [1,2,3]. Up to now no entirely satisfactory solution has been found: the difficulty comes from the complex problem of the estimation of the Doppler shift of the signal frequency due to the relative motion of the detector-pulsar system which leads to an unaffordable amount of computing time.

It is challenging to note that the rotation slow-down of pulsars in binary systems is very significantly smaller than that of isolated ones [4]. This fact suggests that there might be a phenomenon of accretion between the two companions that spins-up the rotating neutron star, compensating partially for its loss of energy by radiation. If this picture is a good hypothesis it means that the amplitude of the gravitational waves emitted by pulsars belonging to a binary system, for instance in X-ray binaries, might be much larger than the amplitude from those emitted by single pulsars, hence the interest for the development of a manageable method aiming at their detection.

In this note we describe a first test of a new strategy aiming at detecting gravitational waves from pulsars in binary system in an all-sky search. We use, for this test, the real data taken by Virgo during the period May 18<sup>th</sup> 2007 – October 1<sup>st</sup> 2007 (VSR1 data)[5] to which we add simulated signals of pulsars in binary systems.

## 2. Data used and pulsars simulation

### Data selection

To test the method, we have selected VSR1 data (hRec V2)[5] sampled at 4096Hz, surviving a few basic cuts:

- Science mode data have been used
- Category 1 cuts have been applied, thus eliminating any interval marked as “crap, do not use this data in any analysis”
- Several higher order cuts has been applied, dropping periods with specific issues, including:
  - saturations of the mirror control signals;
  - failures of the local controls;
  - bad quality or corrupted h-reconstruction;
  - locked segments shorter than 300s;
  - malfunctioning of the global controls;
  - saturations of the second stage of the frequency stabilisation;
  - periods immediately before the loss of a lock;
  - malfunctions of the power stabilisation
- Only segments longer than 1024s have been considered.
- We restrict ourselves to a limited frequency band: 284.-316. Hz.

Despite these cuts, the data retain several disturbances, which make the test entirely representative of future searches on real data.

### Parameters of the simulated pulsar signals

The pulsars' data are taken from the ATNF catalogue [7]. Some of their parameters are listed in Table 1. To limit the computational costs of the test, we've confined the analysis to a sub-band of the VSR1 data, having a width of 32 Hz; therefore the observed frequencies of the pulsars have been shifted in the range 284.-316. Hz.

Pulsar name	Frequency	Generated GW freq. (Hz)	PB (days)	PB (#FT)	A1 (3)	Ecc.	Longitude (deg)	Latitude (deg)
J1915+1606 (1)	16.94	292	0.322	54.33	2.34	0.61	49.97	2.12
J0024-7204H	311.49	295	2.35	396.6	2.15	0.07	-54.1	-44.9
J0024-7204O	378.3	298	0.136	22.95	0.045	0.	-54.1	-44.89
J0024-7204S	353.31	301	1.202	202.8	0.766	0.00039	-54.1	-44.89
J0034-0534 (2)	532.71	304	1.589	268.1	1.438	1.4e-5	111.49	-68.07
J0218+4232	430.46	307	2.029	342.4	1.984	2.22e-5	139.51	-17.53

(1)“Taylor’s pulsar”[6] , (2) Julien Ramonet's Thesis[2] , (3)Projected semi-major axis (light seconds)

Table 1 Summary of the main characteristics of the generated pulsars

The celestial position of these pulsars is sketched on Fig.1; among these six objects, we have focused particular attention on three pulsars located in a globular cluster system: the “Taylor’s pulsar” (because of the high eccentricity value of the binary orbit), the J0034-0534 which has been the subject of some previous studies [2] and the J0218+4232 pulsar arbitrarily.

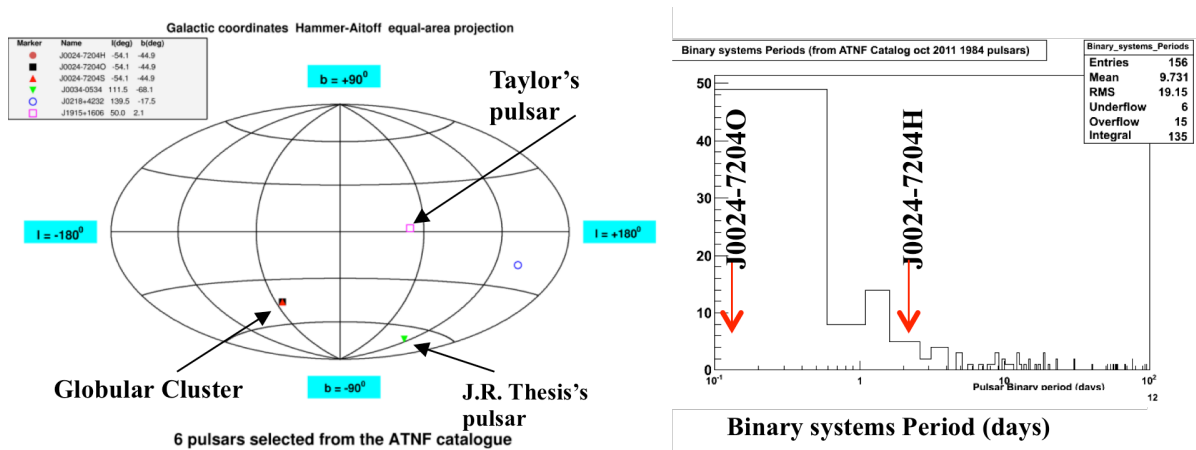


Fig.1 Celestial position of the generated pulsars and distribution of the periods of their binary systems, the selected ones are located between the arrows.

### Details about the signal generation

The simulation of the pulsar signals has been carried out using the SIESTA program [10], particularly a module written by J.Ramonet for simulating signals emitted by pulsars in binary systems [2].

A faster production of data was possible by running the pulsar simulation module at a reduced sampling rate, exploiting the fact that in this way the signal frequency is aliased towards zero frequency, but the signal is otherwise unchanged<sup>1</sup>.

We have generated 5 sets of simulated data for the six chosen pulsars: a summary of the used values is given in Table 2 below; the "h-eff" of the amplitudes quoted in the table are "h effective" values, which take into account the relative orientation of the source and of the detector: fuller details on the estimation of the "h effective" are given in Annex 1.

Pulsar name	Generated GW freq. (Hz)	h-eff Set #5	h-eff Set #4	h-eff Set #3	h-eff Set #2	h-eff Set #1	h-eff Set #0
J1915+1606 (1)	292	7.22e-23	5.78e-23	4.33e-23	2.89e-23	1.44e-23	0.
J0024-7204H	295	6.83e-23	5.46e-23	4.06e-23	2.73e-23	1.37e-23	0.
J0024-7204O	298	6.83e-23	5.46e-23	4.06e-23	2.73e-23	1.37e-23	0.
J0024-7204S	301	6.83e-23	5.46e-23	4.06e-23	2.73e-23	1.37e-23	0.
J0034-0534 (2)	304	6.02e-23	4.81e-23	3.62e-23	2.41e-23	1.20e-23	0.
J0218+4232	307	8.12e-23	6.49e-23	4.87e-23	3.25e-23	1.62e-23	0.

Table 2 – summary of the amplitudes used in the simulation

### Data format

Data have been saved into a "Short Frequency Transform" format, selecting and saving only the frequency interval [286, 314] Hz of the Fourier Transform (FT) of 512s long blocks of data. The adopted format is the same used by the ROG group for storing Nautilus data [8].

### 3. Time/Frequency analysis

In a binary system the apparent frequency of a pulsar signal will present a periodic variation due to the Doppler shift induced by the relative rotation of the two objects. The idea behind the proposed method is to search for such a periodic evolution. On Fig.1 we show the distribution of the periods of the observed binary pulsars systems together with the position of the slower (J0024-7204H) and faster (J0024-7204H) rotating generated systems.

During a relatively short time interval one can expect that the frequency displacement will not be too large, and that the pulsar's frequency will remain inside a single Fourier transform bin; in the following, we have fixed at 512s the time length of the Fourier Transform, which we have verified being safe for the pulsars considered.

The fact that Virgo is not continuously taking data, because of unforeseen instabilities, is another constraint that must be taken into account. In Fig.2 we show the duty cycle during the VSR1 data-taking period. In this histogram the time bins containing "useful" data are set to 1, and those for which either the detector was "off" or the data were unusable were set to 0.

<sup>1</sup> The chosen 32Hz band could in principle be covered by a 64Hz simulation, but this would lead to the frequency interval folding into itself; we have chosen instead to simulate at 128Hz, so that the [284, 316]Hz interval is aliased to the non-overlapping interval [28, 60]Hz.

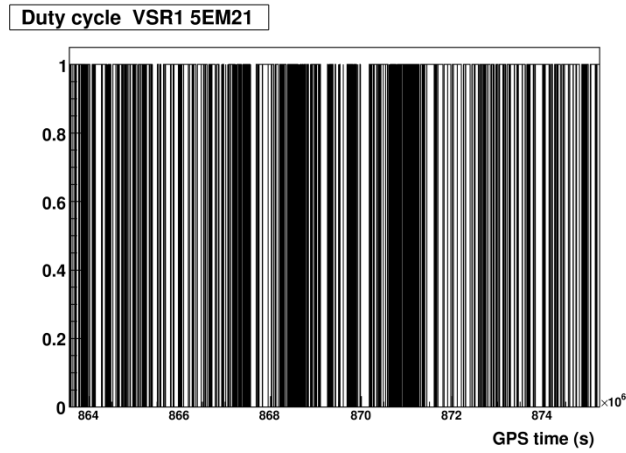


Fig.2 VSR1 data Duty cycle

In Fig.3 we show the spectral density of the VSR1 data + the simulated pulsar signals, assuming an  $h$  value as in Set#5 (maximum amplitude simulated) and Set#0 (zero amplitude): see Table 2 above for the signal's amplitude. The frequencies of the injected pulsar signals are indicated with vertical coloured lines; we can see small peaks, sometimes slightly displaced due to the Earth movement. We note at 300Hz a large peak that is generated by a harmonic of a 50Hz pickup effect.

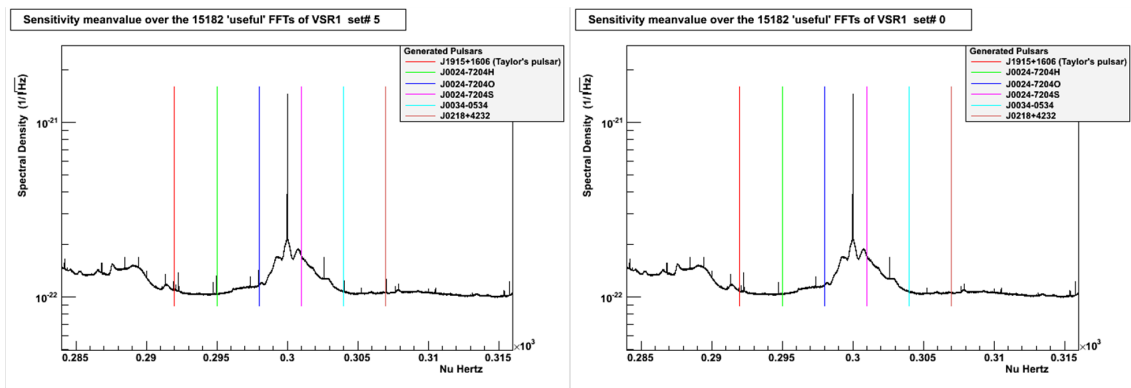


Fig.3 Average spectral density of the VSR1 data in the frequency interval [284, 316]Hz. With a resolution of 1/512Hz, obtained averaging over all available 512s intervals in the data. The pulsar's signal amplitude corresponds to sets 5 (and 0 for comparison)

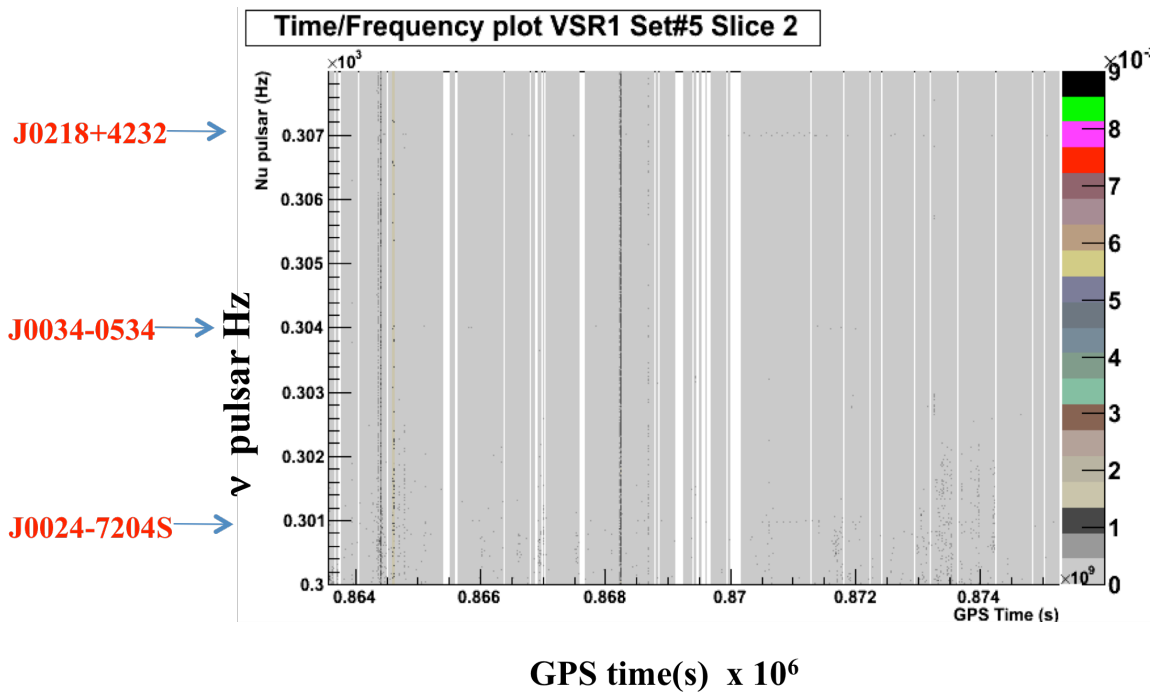


Fig.4 Time/Frequency plot of these data between 300 and 308Hz

In Fig.4 we show the time/frequency plot of the amplitude of the Fourier transform, coded with the color scale shown at the right side of the plot, in a restricted frequency interval [300, 308]Hz. The frequencies of the three pulsars injected in this interval are indicated on the left side; the amplitude of the simulated signals is also in this case the one of Set#5. From this plot, we could detect no significant signal with the naked eye.

#### 4. Principle of the analysis method

We now perform, on the time/frequency plot, an autocorrelation (see annex 2) at fixed frequency, ranging from 284Hz to 316Hz. In Fig.5 we show the 2-D representation of this autocorrelation, restricted to the interval [300, 308] Hz, which includes 3 of the simulated signal frequencies. It is evident the presence of structures which are related to the injected signal.

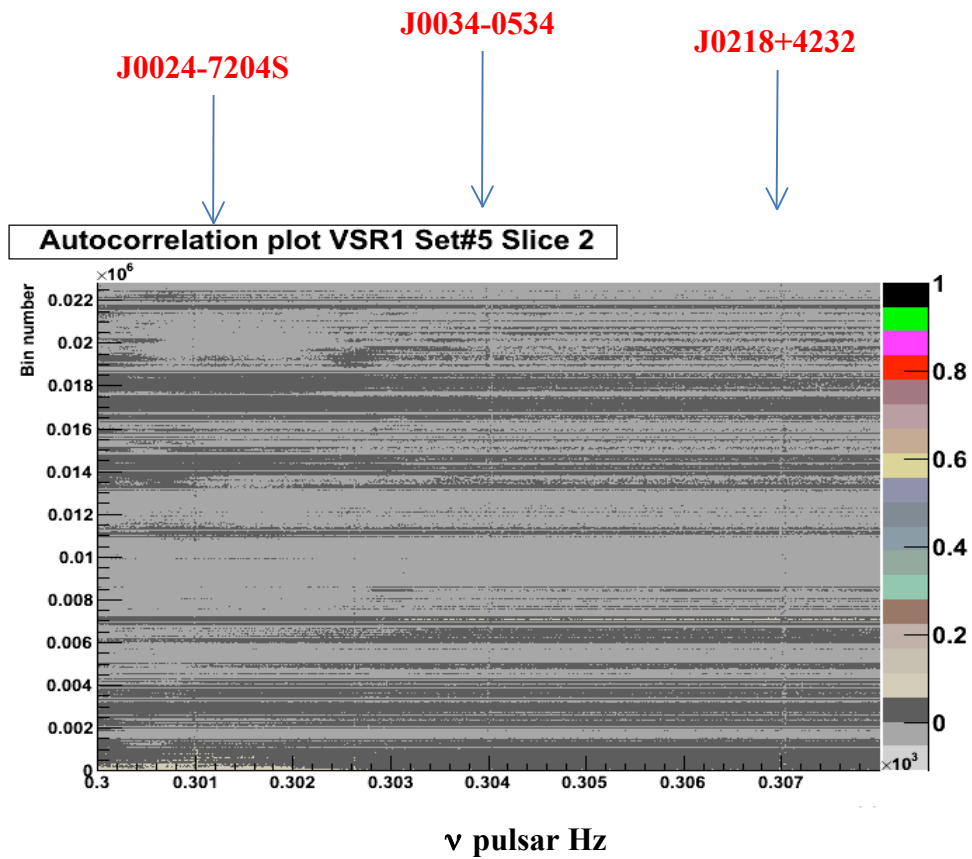
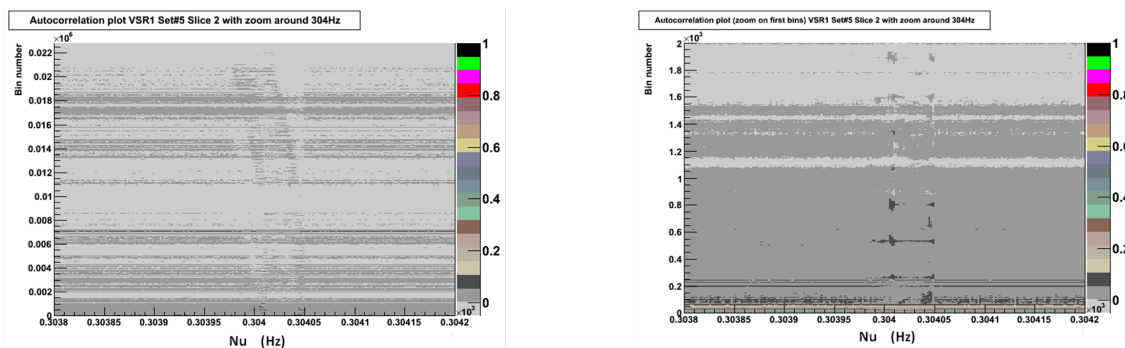


Fig.5

**Characteristics of this autocorrelation plot:**

In order to explain the principle of the method, let us focus on pulsar J0034-0534 that has been studied in a previous work [2] and has been generated here with a 304Hz frequency.



(a) Zoom around 304Hz

(b) same as (a) with a zoom on the 2000 first bins of autocorrelation

Fig.6

If we zoom around 303Hz, in Fig.6 (a) we can see the effect of the Earth rotation; the effect of the binary system rotation is not easy to see because of the quite short period of the system. In Fig.6 (b) looking at the same plot with a zoom on the 2000 first bins of autocorrelation, we see “clearly” the accumulation foreseen in annex 2, indicating the presence of a periodic structure.

Since, when looking at a fixed bin of autocorrelation, there is a structure non uniform along the frequency axis it is natural to look at the evolution as a function of the autocorrelation bin of some characteristic parameters of this structure.

Taking a slice 100 bins wide around 304Hz we compute the RMS (square root of the variance). In fig.7 we show the evolution of this quantity as a function of the bin number.

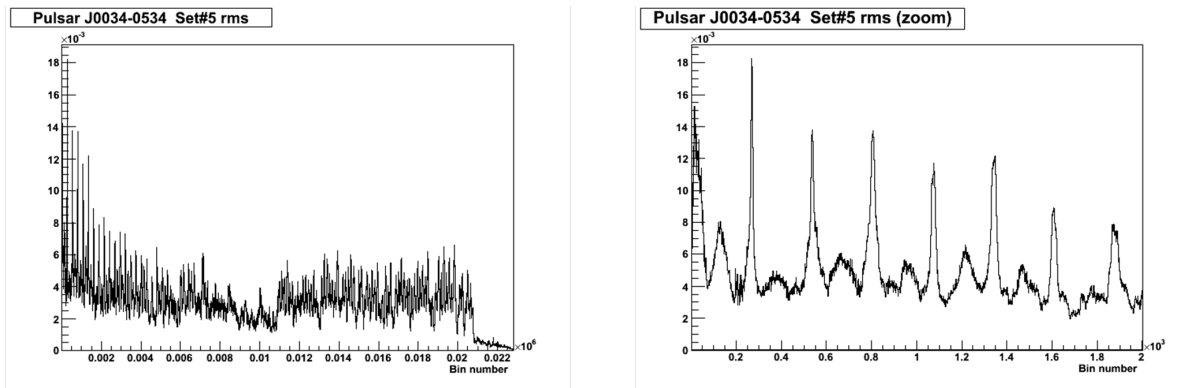


Fig.7 RMS evolution as a function of the autocorrelation bin number, without zoom (left) and with zoom (right)

We observe here a striking structure of peaks separated by the period of the binary system,  $P_b=1.589$  days, which corresponds to 268.2 intervals of 512s.

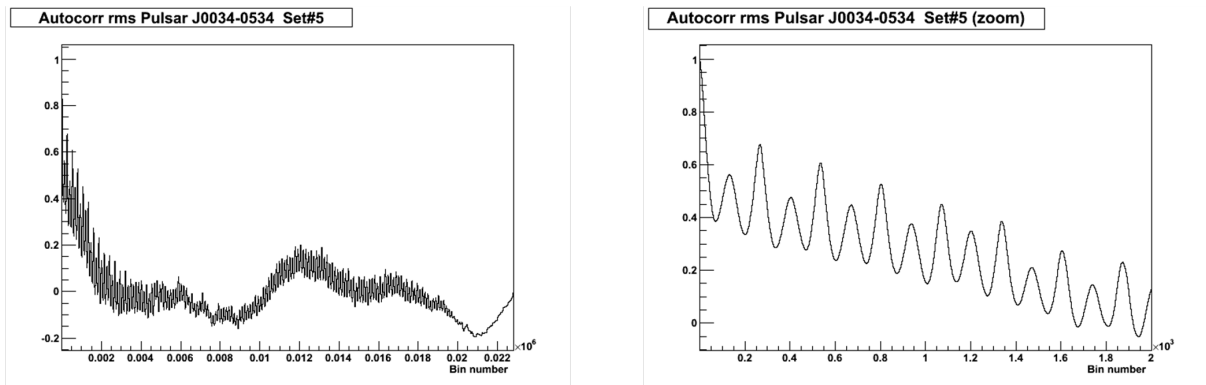


Fig.8 Autocorrelation of the plots shown on Fig.7



On Fig.8 we show the autocorrelation of the RMS evolution as displayed in Fig.7: we see a less spiky structure with clear peaks at the rotation frequency of the binary system accompanied by smaller peaks at double frequency.

For completeness, on Fig.9 and Fig.10 we display the behaviour of the third and fourth moments (skewness and kurtosis), again these quantities present peaks at the binary system period.

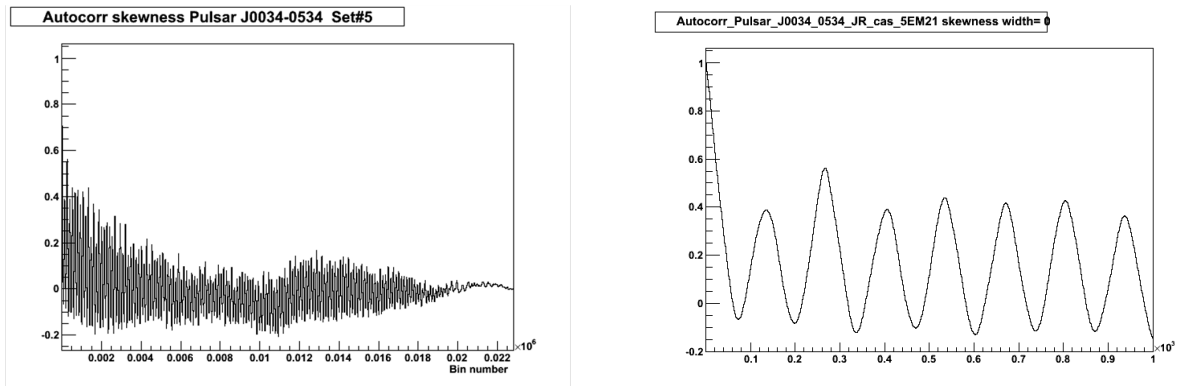


Fig.9 same plots as Fig.8 for the skewness quantity

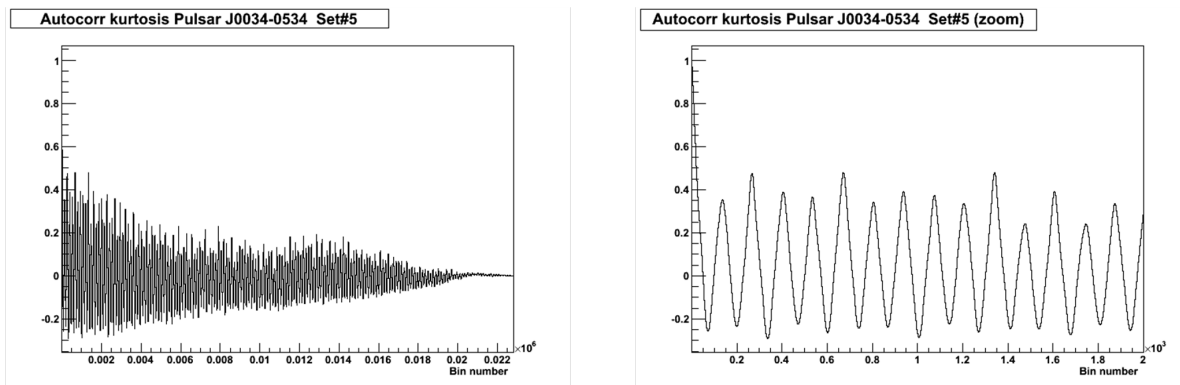


Fig.10 Same plots as Fig.8 for the kurtosis quantity

In this note, we will concentrate only on the RMS evolution.

### Extraction of the binary system period

Extracting the period consists in finding the distance between the maxima in the distribution of the RMS quantity. To our knowledge no mathematical standard tool exists to perform this operation. Since a standard Fourier transform did not give us satisfactory results, we have used an “ad hoc” method that we discuss below.

Here we illustrate this extraction by taking, in the Frequency versus autocorrelation of Fourier transform plane, the RMS value of the autocorrelation, in a slice 100 bins wide in frequency around the generated frequency, for the J1915+1606 pulsar (called here the “Taylor’s pulsar”). The distribution is shown in Fig.11 for the h value of Set#5 (see table 2). We choose

this pulsar because of its challenging properties (a short binary system period and an important value of the eccentricity (0.6) of the system)

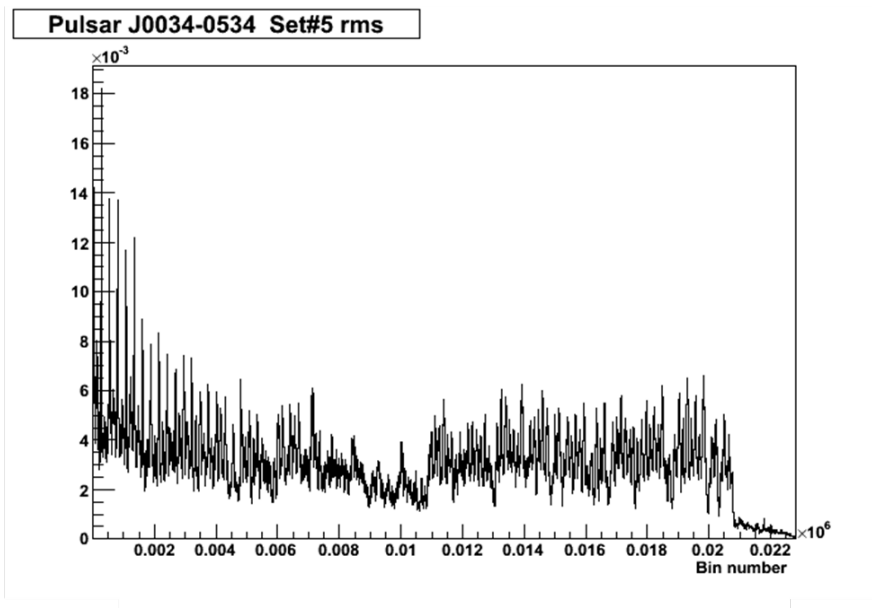
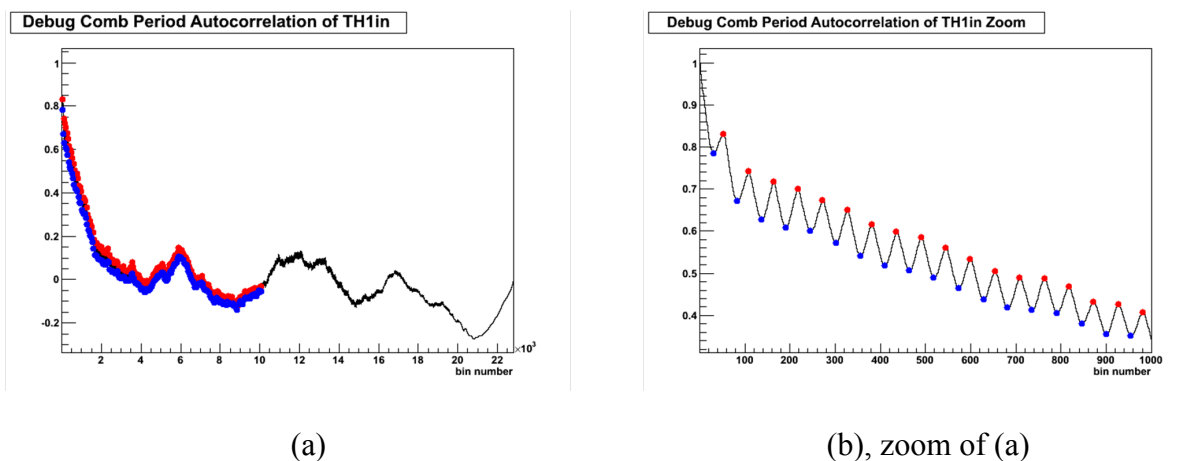


Fig. 11

Since this distribution is quite spiky, we smooth it out by using its autocorrelation; the result is shown in Fig.12 (a) and zoomed in Fig.12 (b). The coloured points are the successive maxima and minima of this autocorrelation, the method used to find these max/min values consist in fitting a parabola over a number of consecutive points (*npfit*), starting at the first point and moving forward looking for a change in the local derivative; the procedure continues up to when a maximum is not followed by a minimum.

This *npfit* quantity is a crucial value since, if it is chosen too large it will not allow the detection of small periods and, chosen too small will lead to problems with small irregularities. This quantity needs therefore to be tuned carefully, anyway for the case at hand we used *npfit* = 10.



(a)

(b), zoom of (a)

Fig.12

Next step is to histogram the distance between two consecutive maxima (red points) and fit a Gaussian shape as shown on Fig.13. The mean value of this Gaussian will give the period of the binary system (in number of Fourier transform) and the maximum will be the number of maxima (quite high in the case of the “Taylor’s pulsar” because of the short period of its system).

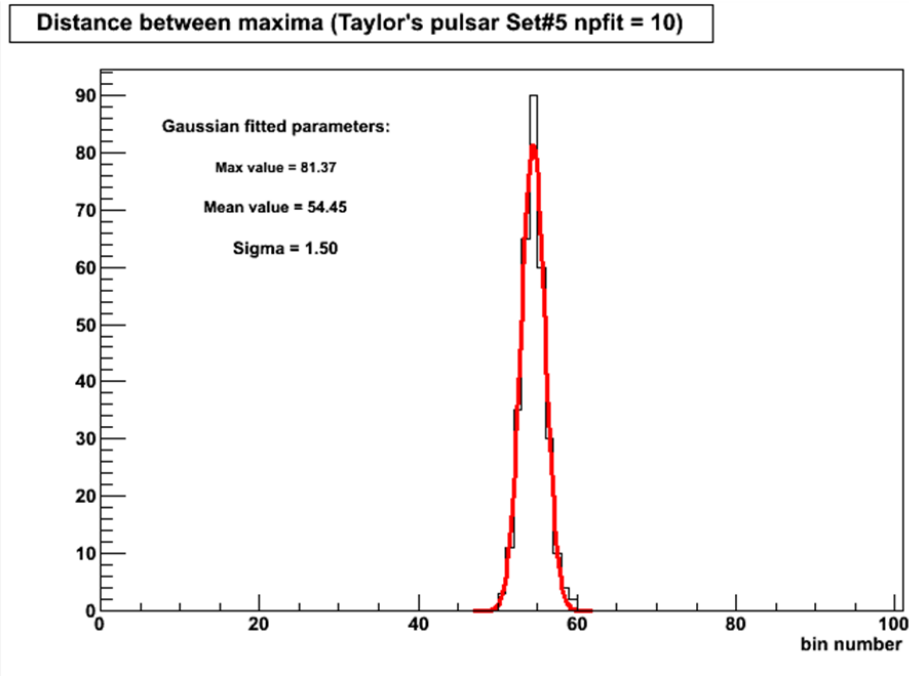


Fig. 13: fit of a Gaussian on the histogram of the distance between two consecutive maxima

Note that the binary system into which the “Taylor’s pulsar” evolves has a period of revolution of 0.322 days, corresponding to 54.33 Fourier transforms of 512s length, very well matching this fit result (54.45).

## 5. Strategy

The idea for a search of a pulsar belonging to a binary system is therefore to scan the frequency domain, bin by bin, using a window of a fixed number of bins centred at the studied frequency. In the previous plots we used a window of 100 frequency bins.

This scan, when the frequency bin do not corresponds to a binary system, will not give a result as striking as those of Fig. 13. A Gaussian shape is expected only when a periodicity is present, its amplitude at the peak is related directly to the number of maxima found, that is the number of periods of the binary system. When the window do not contain “Gaussian-like” data the fit become meaningless, Therefore we cut out (reset the bin content of the scan) in the following cases:

- The fitted gaussian amplitude  $C_0$  is lower than 2 (we must have more than 2 binary periods to detect a binary system)
- The fitted gaussian amplitude  $C_0$  is higher than 1000 (corresponds in the VSR1 case to a period of less than 0.1 day)
- The fitted Gaussian amplitude  $C_0$  is lower than its fitted error
- The fitted RMS of the found Gaussian is negative
- The fitted RMS of the found Gaussian is larger than 200 (2 times the total width of the running window)

These cuts are imposing quite weak constraints, we use them instead of a global chisquare cut less intuitive to understand.

An important parameter of the search is the width of this running window. We illustrate this on Fig. 14, where we show the evolution, as a function of the autocorrelation bin number, of the RMS of the data located inside the window along the frequency axis at fixed autocorrelation bin, in the case of the generated J0034-0534 pulsar.

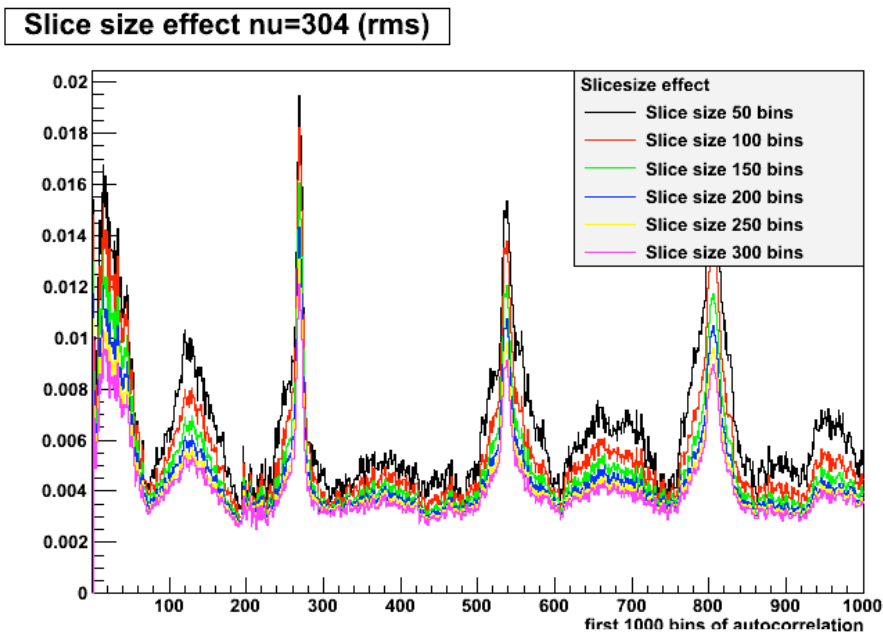


Fig. 14: we show here, for the Set #5, at the frequency  $\nu=304$  Hz, the effect on the RMS of choosing a different size for the slice, displaying the first 1000 bins

On Fig. 15 is shown the same data after autocorrelation.

### Slice size effect nu=304 autocorr 1 times after AC

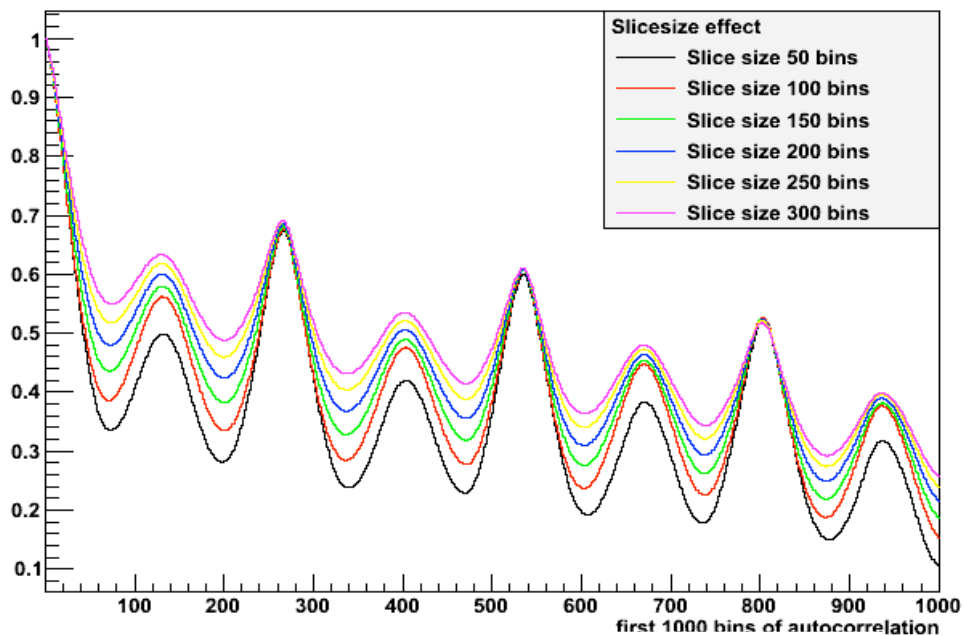


Fig. 15: on the same Set #5 data, at  $\nu=304$  Hz, we show the same effect on the autocorrelation of the RMS, for different values of the slice size.

We clearly see that the window width has an important effect upon the signal over noise ratio; therefore the value of this parameter will also need to be optimized before using extensively this method. Since the value of 100 bins gives good results, we will use it throughout this work.

Another important parameter is the value of *npfit*, the number of points taken into account when fitting a parabola in order to find the max/min values as discussed before. In order to be “safe” we have performed the bin by bin scan using 5 different values namely 5, 10, 15, 20 and 40 points. These values are aimed at covering the periods of the generated pulsars, which range from 0.136 to 2.35 days.

## 6. Sensitivity

### 6.1 - Sensitivity versus simulated h

It is crucial to study the sensitivity of this method to the amplitude of the signal (the “h” value) and to the amount of data used. Using, as an indicator, the maximum of the fitted Gaussian (see Fig.13), we perform a scan along the frequency. Since we do not know “a priori” the binary system frequency, we add the scan results for each of the 5 *npfit* values mentioned above; moreover, in order to smooth the peaks in the results we perform an ideogram[9] of the scan. In Fig.16 is displayed the results for five generated amplitudes (see table 2)

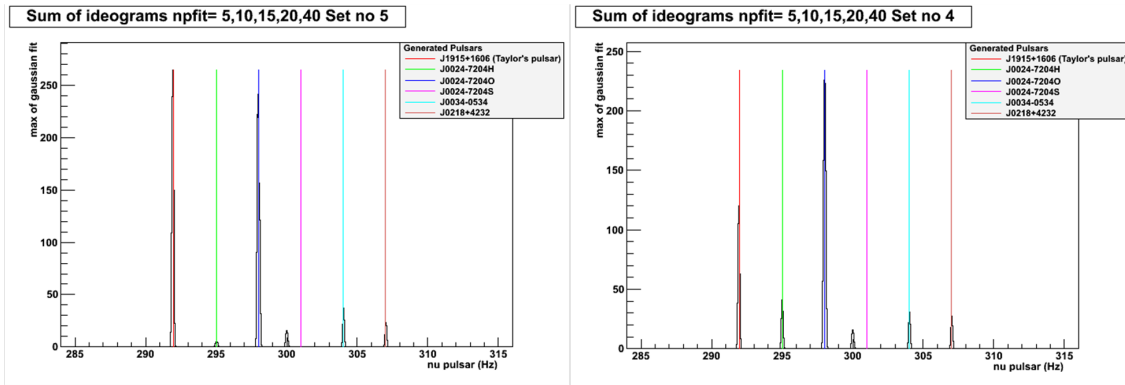


Fig.16(a) Maximum of Gaussian fit, generated h is from Set#5 and Set#4

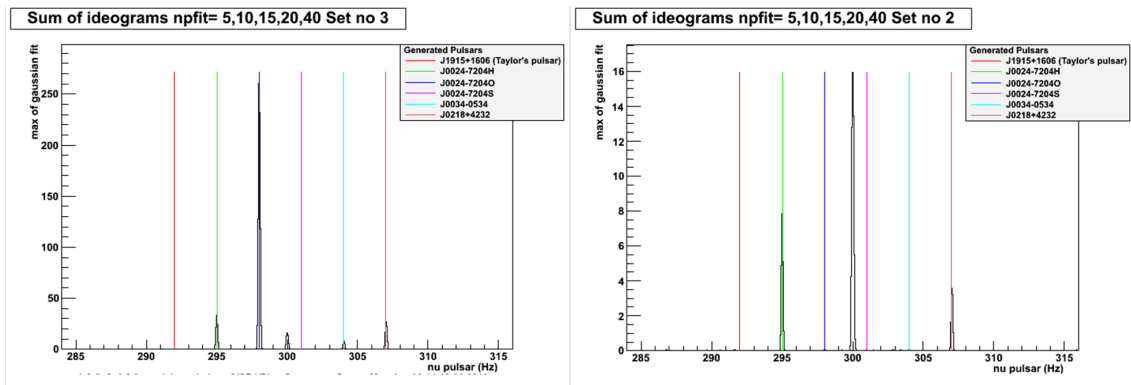


Fig.16(b) Maximum of Gaussian fit, generated h is from Set#3and Set#2

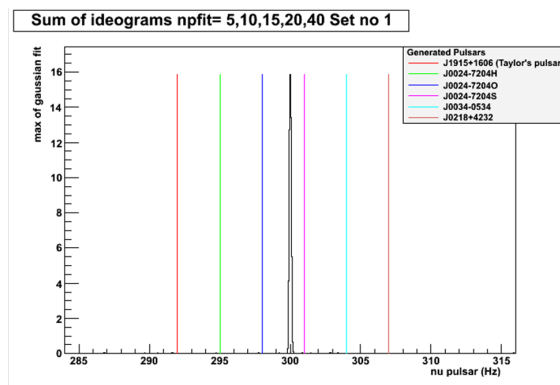
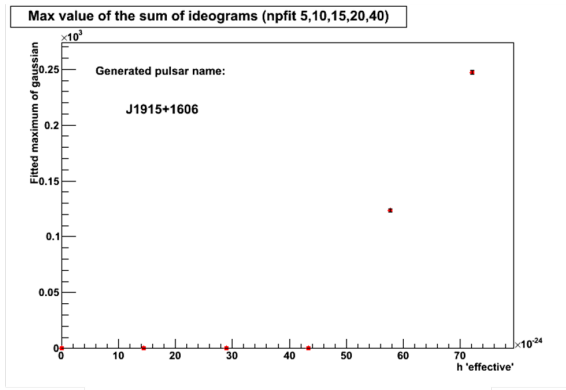
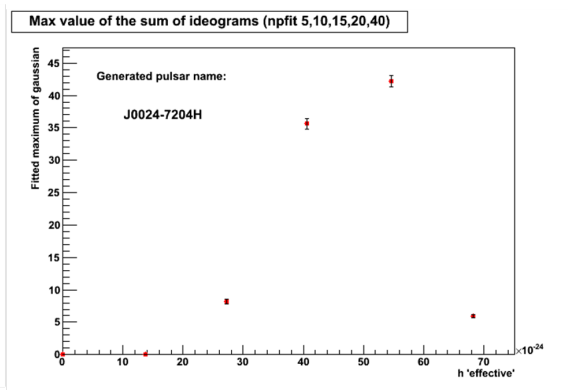


Fig.16(c) Maximum of Gaussian fit, generated h is from Set#1

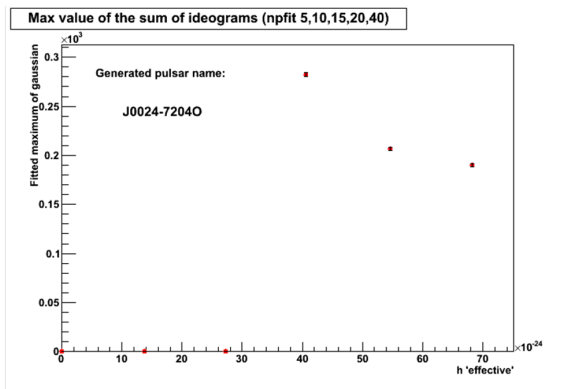
For each set of generated values we plot the maxima found in a window of  $\pm 0.4\text{Hz}$  around the generated pulsar's frequencies, the results are displayed in Fig.17a to Fig.17f



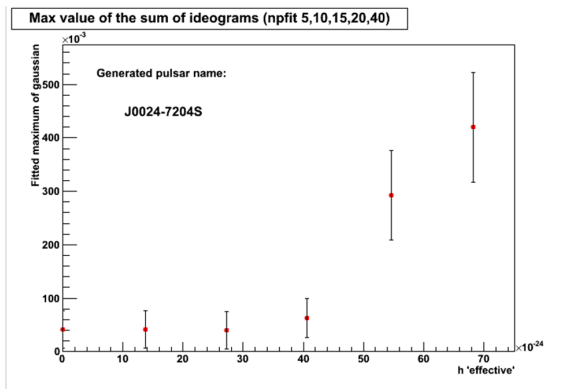
(a)



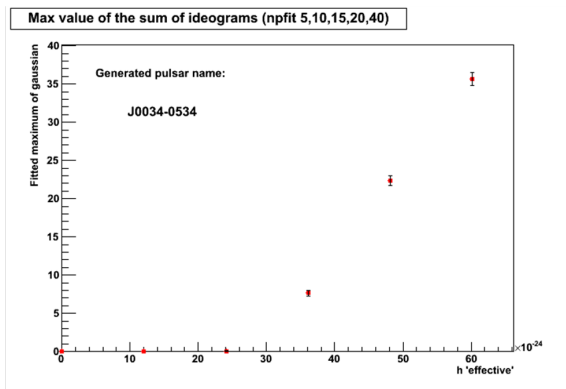
(b)



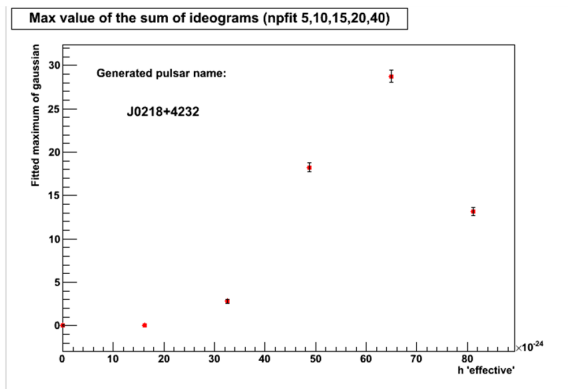
(c)



(d)



(e)



(f)

Fig. 17 Maxima as a function of the generated  $h$  value for the six generated pulsars. The errors are only the statistical errors of the  $\chi$ -square fit.

We see that the behaviour depends strongly of the pulsars parameters.

## Sensitivity versus amount of data

In order to obtain an idea of the evolution of the signal as a function of the accumulated statistics, we have repeated the exercise using only a fraction of the VSR1 data. We use the Set#5 data for the simulation and use 100%, 80%, 60%, 40%, 30% and 20% of the data. These percentages are taken from the beginning of VSR1.

In the same way, as above for the h values, we plot the corresponding maxima and mean values on Fig. 18(a) to Fig. 18(f)

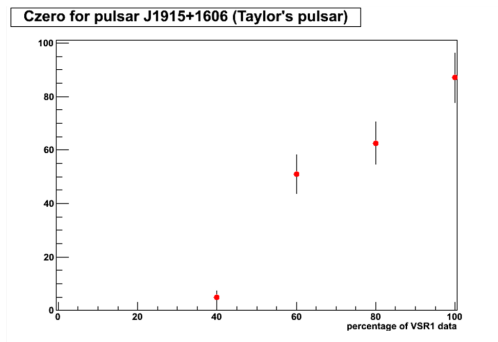


Fig. 18(a1)

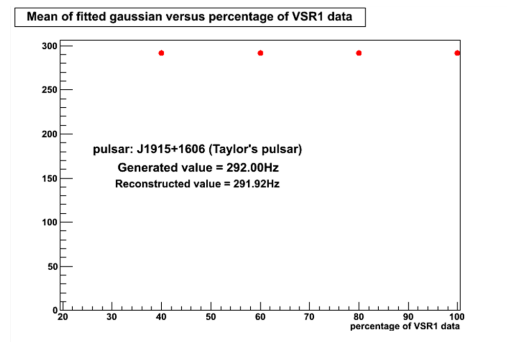


Fig. 18(a2)

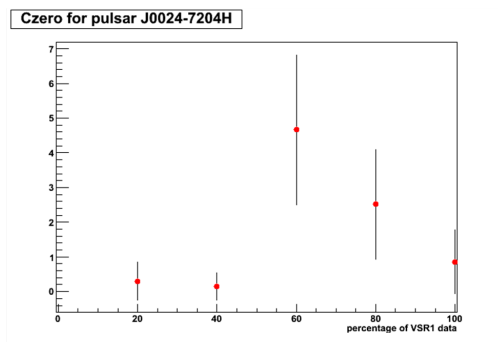


Fig. 18(b1)

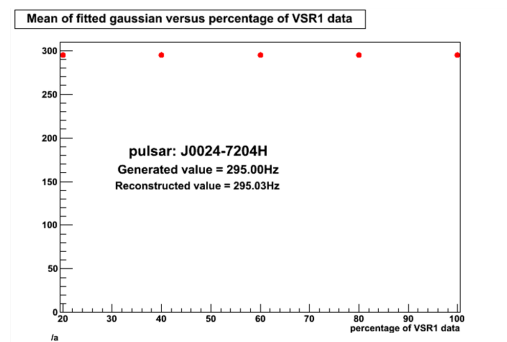


Fig. 18(b2)

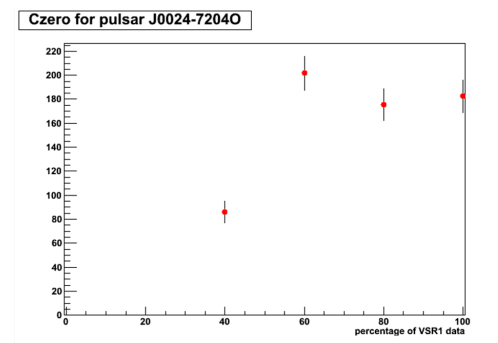


Fig. 18(c1)

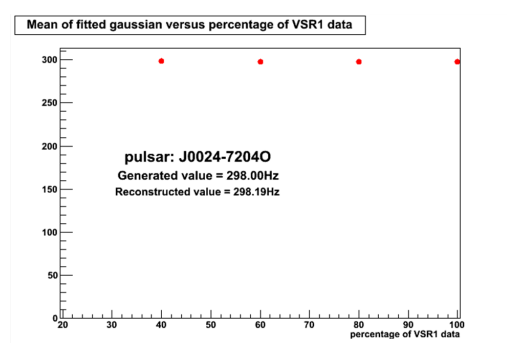


Fig. 18(c2)



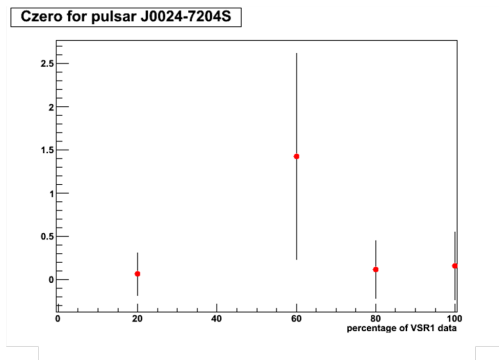


Fig. 18(d1)

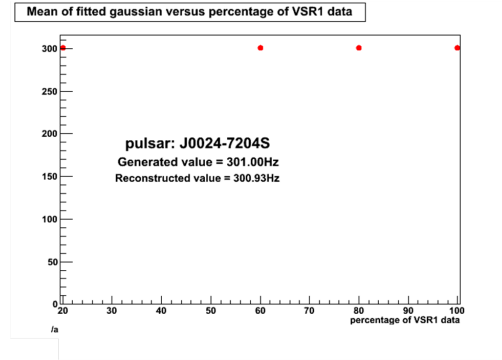


Fig. 18(d2)

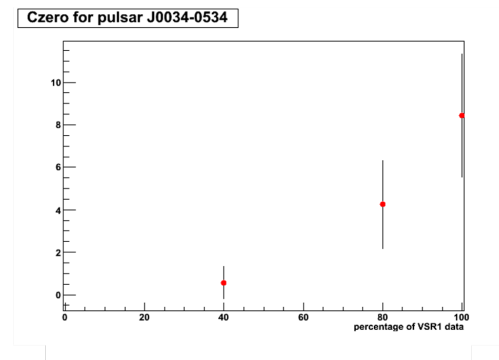


Fig. 18(e1)

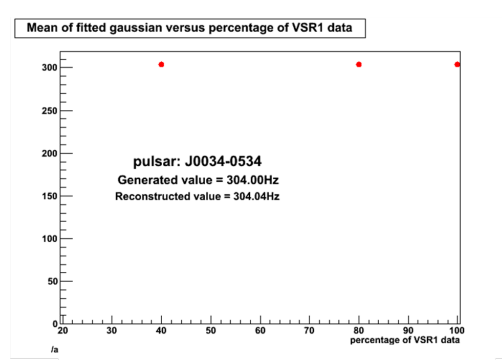


Fig. 18(e2)

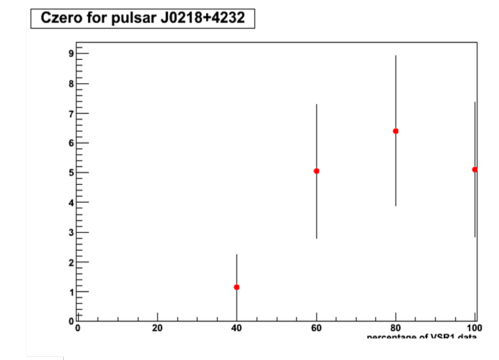


Fig. 18(f1)

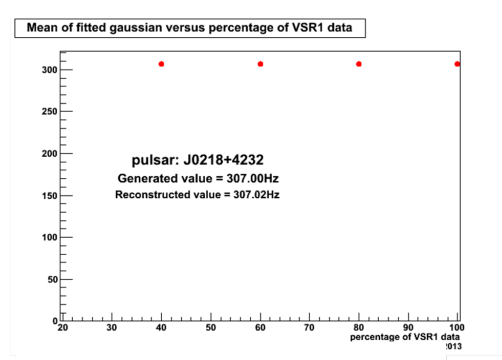


Fig. 18(f2)

Here again, the evolution as a function of the statistics used is a strong function of the pulsars parameters. We see that even with half of the VSR1 data, almost all the generated pulsars are found with the initially generated parameters.

### Computing time

All the calculations performed here were done at the Lyon computing centre [12]; the estimation of the computing time used is not trivial since the batch system used in Lyon does not schedule always processors of the same power to the jobs. Actually we use 32 processors at the same time, for a given percentage of the VSR1 data, hence we have chosen to histogram the mean value of the “normalized computing time” given for each job and then

take the mean value as the CPU time value and its RMS as the error (beware this is not the true error!). The result is summarized on Fig. 19, the line shown on this graph corresponds to a linear fit performed using the points above 30% of the total VSR1 data.

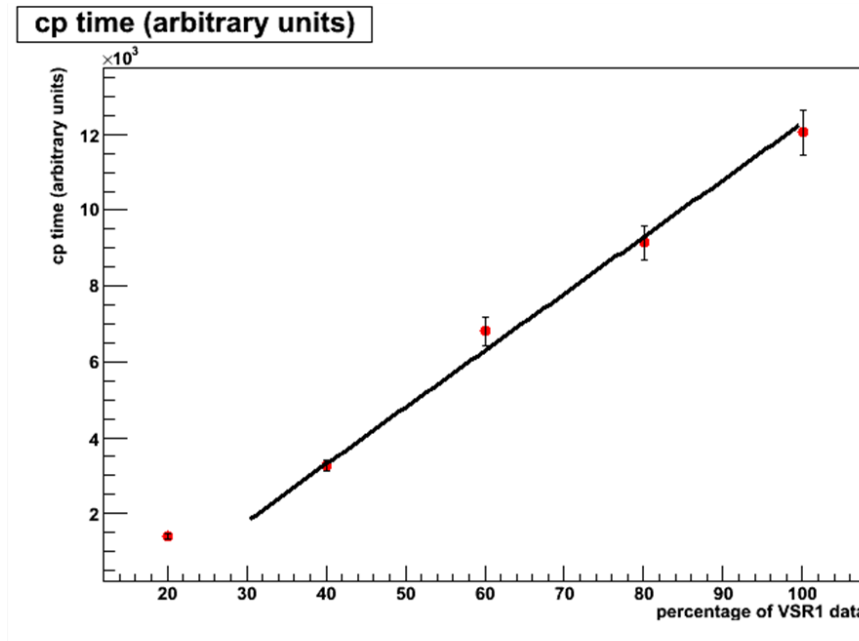


Fig.19: Mean computing time versus the percentage of VSR1 data

We clearly see that, above 30% the computing time used is nicely following a linear increase with the amount of data.

## Outlook and discussion

This first tentative of a moments autocorrelation method aiming at the detection of pulsars belonging to a binary system clearly needs further work before becoming fully operational. Even if not yet mature, it shows several encouraging properties since the computing time needed is increasing almost linearly with the amount of data. The sensitivity is promising since, comparing Table 2 and Fig. 17 (a)-17(f) we see that even with less than 50% of the VSR1 data set a sensitivity of  $h \approx 5 \cdot 10^{-23}$  is reached even for the pulsar J0024-7204S which has been generated at 301Hz, where the noise is quite higher than for the others.

Further work is needed before reaching an operational status, namely an optimization of several parameters (like the scanning window width and the *npsfit* parameters that we have described before). An improvement of the search method concerning the identification of the period of the binary system is also needed (we have only used a very coarse method here), a new robust mathematical tool need to be developed. An evaluation of the acceptance versus the parameters of the binary system (period, angles of the orbital plane, semi-major axis and eccentricity of the system...) should also be carried out. Another improvement that might be very powerful is to combine this search, up to now based only on the RMS evolution, with the

skewness and kurtosis behaviour, these quantities being weakly correlated between themselves should bring new information and therefore a better sensitivity of the method.

Since the amplitude of the gravitational waves expected from binary pulsars is, up to now, not reasonably predictable, in principle it might be much larger than the one of isolated pulsars, hence we think that it is very important to undertake a full search using all the available data (Virgo + LIGO). Such a search will give “seeds” (starting values of the pulsar frequency and period of the binary system) for more sophisticated and computer time demanding methods.

## Acknowledgements

We would like to warmly thank the members of the Annecy-LAPP team, particularly F.Marion for her help in using the SIESTA[10] simulation package, D.Buskulic and L.Rolland for helping with the use of the ROOT[11] data analysis package and B.Mours for pointing out an unnoticed normalization mistake.

One of us (MY) has specially appreciated several enlightening discussions about signal processing with Philippe Bolon (Université de Savoie).

## References

[1] M.Yvert for the Virgo Collaboration, *A first test of a sine-Hough method for the detection of pulsars in binary systems using the E4 Virgo engineering run data*, Class. Quantum Grav. **21** (2004) S717-S727, [5<sup>th</sup> Edoardo Amaldi Conference on Gravitational Waves (2003)]

[2] Julien Ramonet thesis: *Étude de méthodes d'analyse en vue de détecter les ondes gravitationnelles émises par des pulsars avec l'interféromètre Virgo*  
Université de Savoie, 29 août 2003

[3] S van der Putten, H J Bulten, J F J van den Brand and M Holtrop, *Searching for gravitational waves from pulsars in binary systems: an all-sky search* J. Phys.: Conf. Ser. **228** (2010) 012005 [ 8<sup>th</sup> Edoardo Amaldi Conference on Gravitational Waves (2009)]

[4] This property has been noticed and discussed by many authors: see for example D.R. Lorimer, *Binary and Millisecond Pulsars at the new Millennium*, Living Reviews in Relativity **4** (2001) 5.

[5] R.A. Hulse and J.H. Taylor. *Astroph. Journal* **195** (1975) L51-L53.

[6] The Virgo Collaboration, *Virgo calibration and reconstruction of the gravitational wave strain during VSRI*, J. Phys. Conf. Series **228** (2010) 012015.

[7] ATNF Pulsar Group Catalog; for an updated catalog see: Manchester, R. N., Hobbs, G. B., Teoh, A. & Hobbs, M., *Astron. J.* **129** (2005) 1993-2006, astro-ph/0412641  
<http://www.atnf.csiro.au/research/pulsar/>

[8] We have the pleasure to thank S. Frasca, P. Astone and the ROG group in Rome for several constructive discussions.

[9] Here we define an ideogram as a histogram where each bin is replaced by a Gaussian with the same surface and a given resolution, this is an old fashioned trick used to smooth out spiky distributions.

[10] B.Caron et al, *SIESTA: a time domain, general purpose simulation program for the VIRGO experiment*, *Astroparticle Physics* **10** (1999) 369.

[11] ROOT A data analysis framework <http://root.cern.ch>

[12] CNRS Computing Center in Lyon <http://cc.in2p3.fr>

# Annex 1

## Determination of “h effective”

The h value at detector level, as simulated by SIESTA, depends of the celestial position of the pulsar system, and changes over time with the relative orientation of the source and the detector. In order to study the sensitivity of the moment method, we need to know its response for several signal amplitudes. In order to quantify the strength of the signal, we have found useful to define a value of “h effective”, for each generated pulsar, as follows:

We generate a chunk of noise free data, 1 second long, sampled at 1kHz. As an example, on Fig1a and 1b we show the result for the pulsar J1915+1606 (the Taylors’ pulsar)

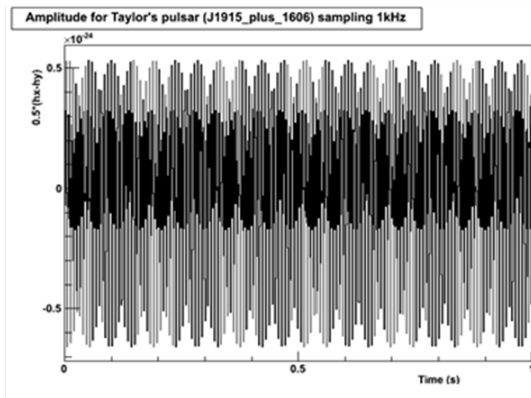


Fig1a - 1second of generated signal

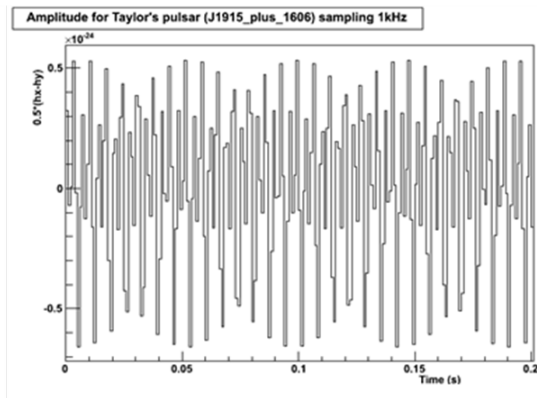


Fig1b – same as 1a with a zoom on 200ms

Taking the maximum value of this generated signal, we plot it as a dot in the following drawings.

Using the input parameters of Table 1A and 1B, we have generated for each selected pulsars 500 sets of amplitude versus time, distributed along the VSR1 data taking time, setting the pulsar's amplitude in the simulation at  $h=1.e-22$  (hvalue in Table 1A)

Pulsar name	Generated Rotation freq. (Hz)	hvalue	alpha	delta	psi	j	gamma
J1915+1606	146.	1.e-22	1.89028	0.279603	.45	.13	.1
J0024-7204H	147.5	1.e-22	0.105207	-1.257834	.45	.13	.1
J0024-7204O	149.	1.e-22	0.105058	-1.258061	.45	.13	.1
J0024-7204S	150.5	1.e-22	0.105009	-1.258006	.45	.13	.1
J0034-0534 (2)	152.	1.e-22	0.149940	-0.097334	.45	.13	.1
J0218+4232	153.5	1.e-22	0.602600	0.742432	.45	.13	.1

Table1A - Binary Pulsar parameters

Pulsar name	PB(days)	a1sini	ecc	omega0	omegadot	tau
J1915+1606	0.322997	2.34177	0.617134	0.	0.	50315.378906
J0024-7204H	2.357697	2.152823	0.07	0.	0.	51000.972656
J0024-7204O	0.135974	0.045153	0.	0.	0.	50000.
J0024-7204S	1.201724	0.766274	0.	0.	0.	50000.
J0034-0534 (2)	1.589282	1.437765	0.	0.	0.	49550.703125
J0218+4232	2.028850	1.984400	0.	0.	0.	49150.609375

Table1B - Binary orbit parameters

The evolution of these maxima is shown on Fig 2a and Fig 2b for the same pulsar J1915+1606.

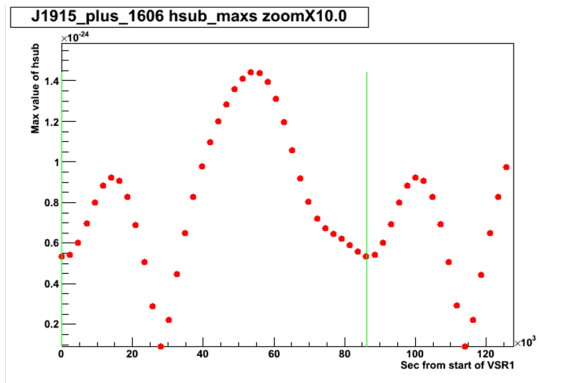


Fig2a

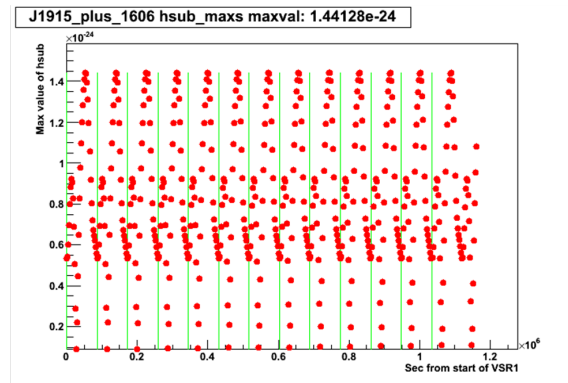


Fig2b (smaller zoom)

A dot in these figures represents the value of the maximum value of a 1s chunk of data at a given time, The distance between vertical green lines is one sidereal day.

We have repeated the same procedure for each selected pulsar, generating 500 sets of amplitude versus time sets, equally distributed along the VSR1 data taking time, with simulation parameter  $h=1.e-22$ .

The corresponding evolution of the maxima is displayed on Fig3 to Fig8

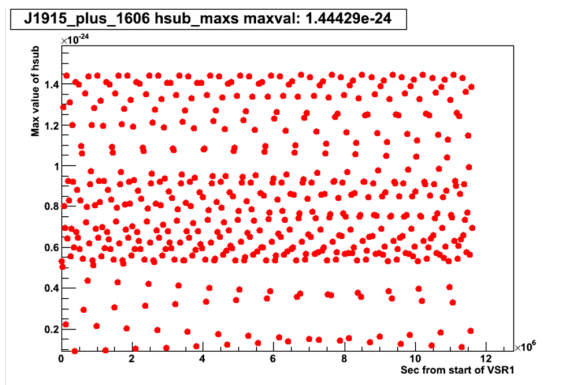


Fig3 pulsar J1915+1607

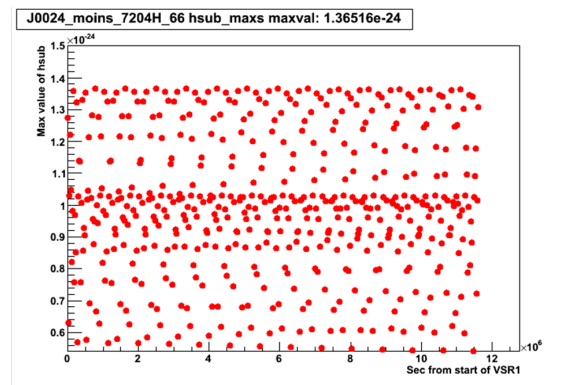


Fig4 pulsar J0024-7204H

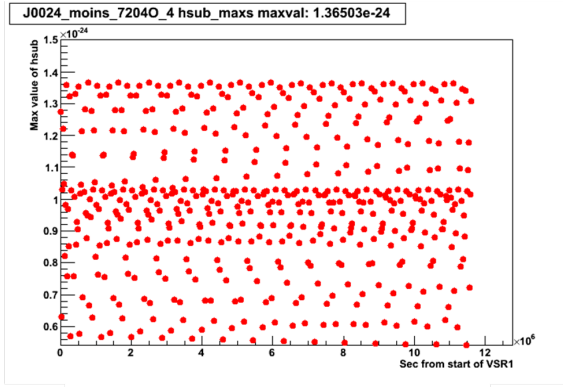


Fig5 pulsar J0024-7204O

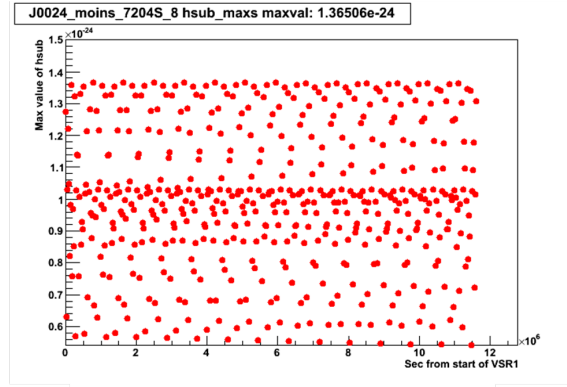


Fig6 pulsar J0024-7204S

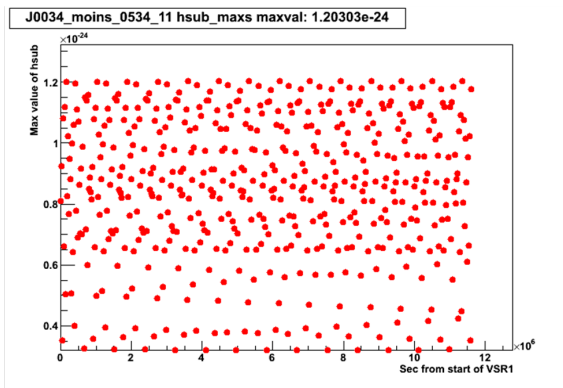


Fig7 pulsar J0034-0534

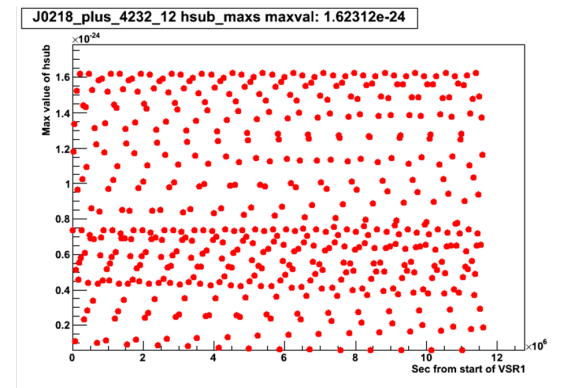


Fig8 pulsar J0218+4232

Taking the maximum value among all these values, we call it the “effective h”, or "h-eff" at detector level.

The table below is a summary of the found values for the given simulated amplitude  $h=1.e-22$

Pulsar name	Generated Rotation freq. (Hz)	Generated GW freq. (Hz)	Effective h
<b>J1915+1606</b>	<b>146.</b>	<b>292</b>	<b>1.444e-24</b>
<b>J0024-7204H</b>	<b>147.5</b>	<b>295</b>	<b>1.365e-24</b>
<b>J0024-7204O</b>	<b>149.</b>	<b>298</b>	<b>1.365e-24</b>
<b>J0024-7204S</b>	<b>150.5</b>	<b>301</b>	<b>1.365e-24</b>
<b>J0034-0534</b>	<b>152.</b>	<b>304</b>	<b>1.203e-24</b>
<b>J0218+4232</b>	<b>153.5</b>	<b>307</b>	<b>1.623e-24</b>

Table2 - “effective h” for the generated pulsars (with parameters from Table1A and 1B)

## Annex 2

### Autocorrelation function

Since the definition of the autocorrelation function is not unique in the literature, we provide in this section the definition of the function we use and list some of its properties

### Definitions

#### Correlation coefficient:

Let  $\vec{x}$  and  $\vec{y}$  be two vectors of N elements,  $\vec{x}(x_1, x_2, \dots, x_N)$ ,  $\vec{y}(y_1, y_2, \dots, y_N)$ , the correlation coefficient between  $\vec{x}$  and  $\vec{y}$  is given by:

$$\rho(\vec{x}, \vec{y}) = \frac{\text{cov}(\vec{x}, \vec{y})}{\sigma_x \sigma_y}$$

Where  $\text{cov}(\vec{x}, \vec{y})$  is the covariance between  $\vec{x}$  and  $\vec{y}$

$$\text{cov}(\vec{x}, \vec{y}) = \frac{1}{N} \sum_{i=1}^N (x_i - \bar{x})(y_i - \bar{y})$$

$\sigma_x$  is the square root of the variance

$$\sigma_x^2 = \text{cov}(\vec{x}, \vec{x}) = \frac{1}{N} \sum_{i=1}^N (x_i - \bar{x})^2$$

#### Autocorrelation function:

The autocorrelation at lag h of vector  $\vec{y}$  is given by

$$r_h = \frac{c_h}{c_0}$$

Where  $c_h$  is the auto-covariance function :

$$c_h = \frac{1}{N} \sum_{t=1}^{N-h} (y_t - \bar{y})(y_{t+h} - \bar{y})$$



$c_0$  is the variance :

$$c_0 = \frac{1}{N} \sum_{t=1}^N (y_t - \bar{y})^2$$

## Some properties of the autocorrelation function

### 1-dimensional example :

Let  $\bar{y}$  be N values of the sinusoidal function  $y = \sin(2\pi vt)$ , sampled at equidistant intervals of time

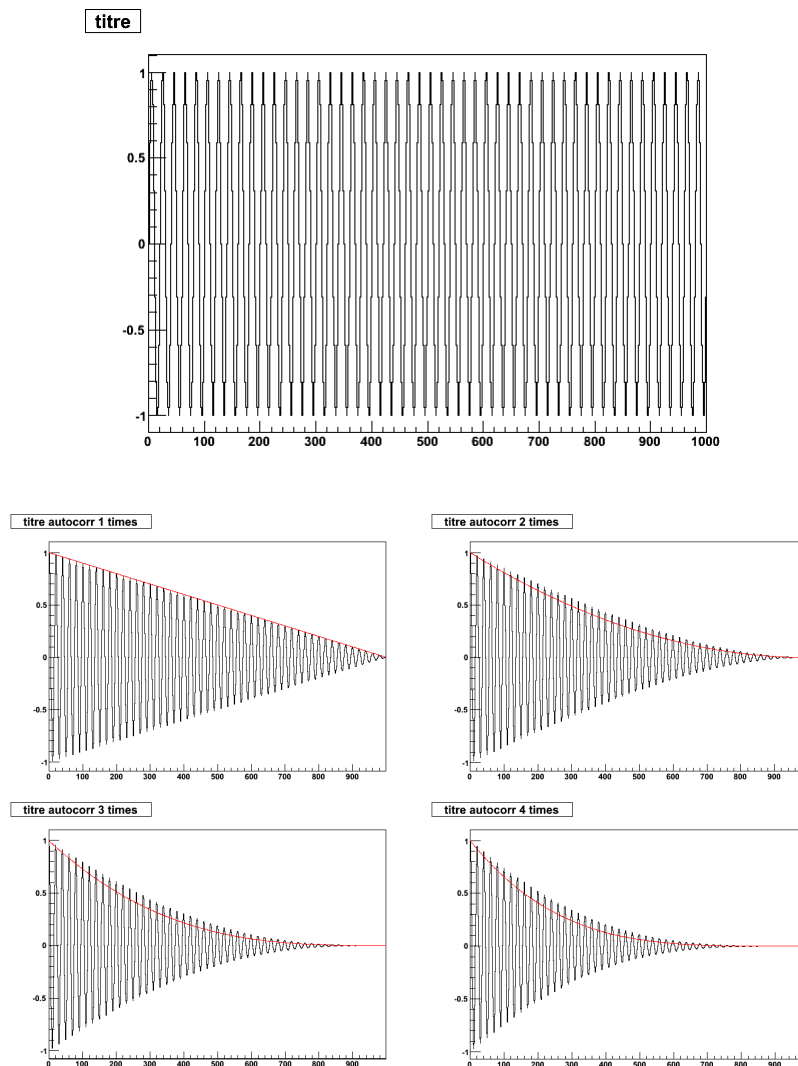


Fig. A1

On fig.A1 is shown the function  $y$  together with its autocorrelation function at several levels.

Level 1 is the simple autocorrelation, level 2 is the autocorrelation of the autocorrelation function, and so on. The curve drawn on these plots are simple polynomials of power  $n$  for level  $n$ , they are meant only to guide the eye.

An interesting property of this autocorrelation function is that, in the case of missing data, it smooths the shape of the data while keeping its maxima at the period of the original function as shown in fig.A2

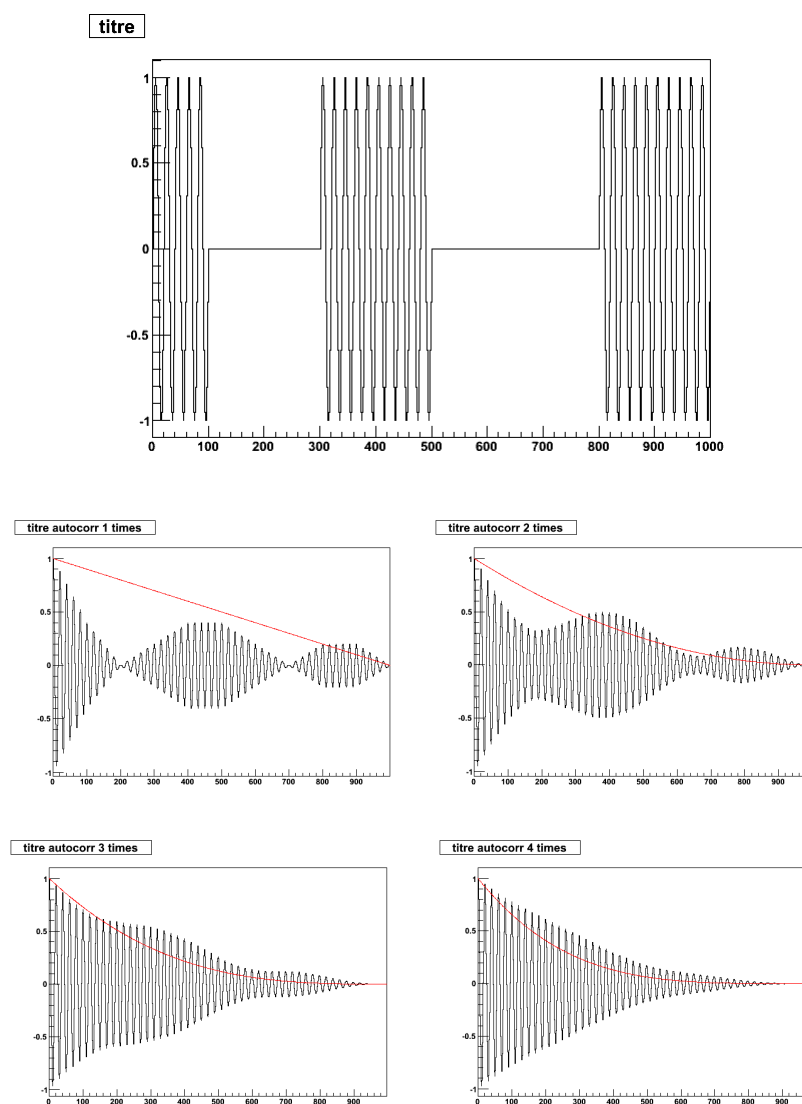


Fig.A2

## 2-dimensional example:

Taking a sine function, let us take the intersections at fixed Y ( $Y=0.6$ )

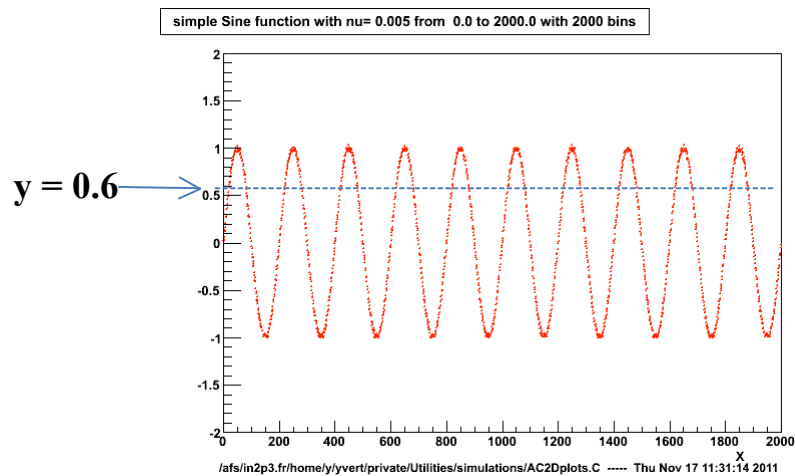


Fig.A3-a

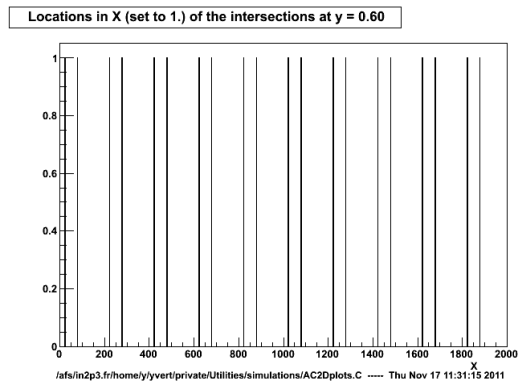


Fig.A3-b

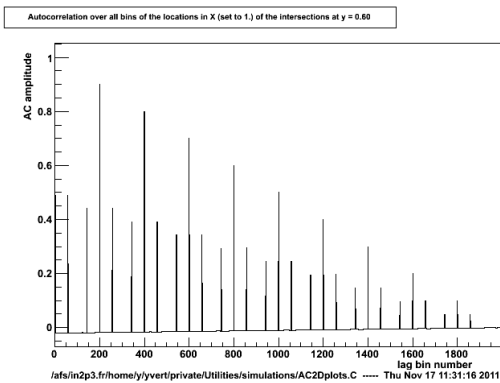


Fig.A3-c

On fig.A3-a, is shown the sine function.

On fig.A3-b, is shown the positions of the intersections of a line  $Y=0.6$  with the sine function.

On fig.A3-c, is shown the result of the autocorrelation of these intersections.

If we do the same operation for all Y values and plot the amplitude of the autocorrelation function versus time we got the result displayed on Fig.A4

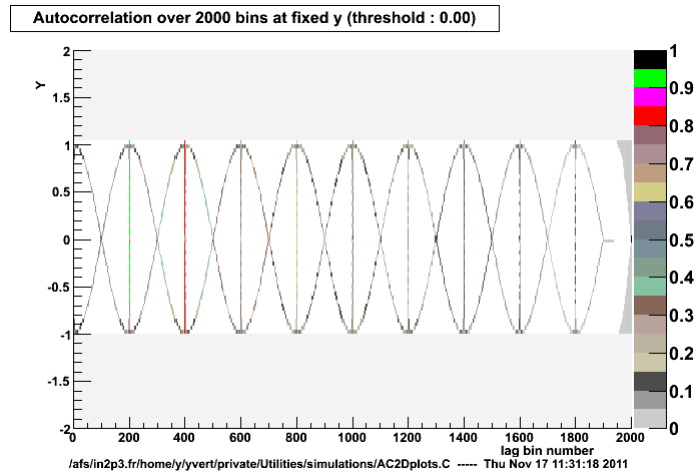


Fig.A4

We clearly see the periodic structure in the autocorrelation plot with the same period as the original sine function

Now we can introduce some random noise added to the sine shape and perform the same autocorrelation, this is displayed on fig.A5 below with 40000 points of noise

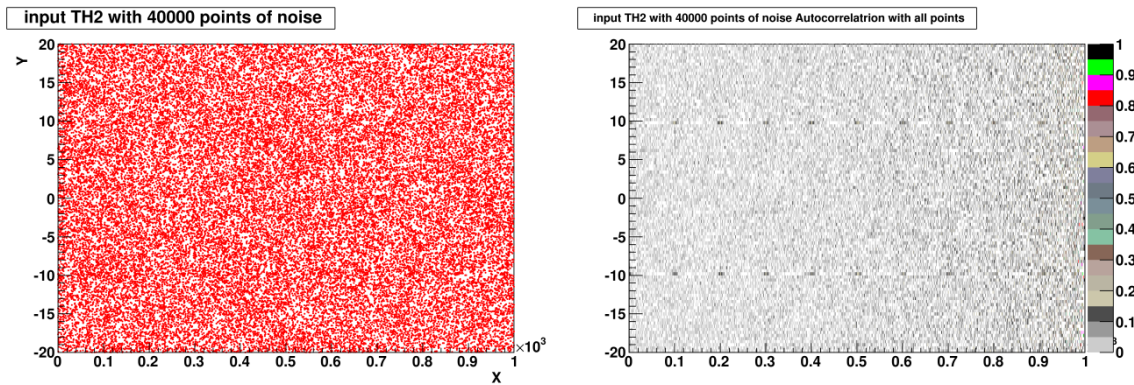


Fig.A5

Even if the sine shape is invisible to the naked eye, we see that the autocorrelation plot keeps the periodic structure of the input signal.